Atmospheric Pollution Research 6 (2015) 45-51

Technical Note

Atmospheric Pollution Research

www.atmospolres.com

Microwave assisted catalytic removal of elemental mercury from flue gas using Mn/zeolite catalyst

Zaishan Wei, Yuwei Luo, Baoren Li, Zhouyang Cheng, Jianbin Wang, Qihong Ye

School of Environmental Science and Engineering, Sun Yat–Sen University, Guangdong Provincial Key Laboratory of Environmental Pollution Control and Remediation Technology, Guangzhou 510275, China

ABSTRACT

The integrated microwave with Mn/zeolite and ozone (MCO) and combined microwave with Mn/zeolite (MC) was employed to oxidize elemental mercury (Hg^0) in simulated flue gas. The results show that mercury removal efficiency attained 35.3% in the MC, over 92% of Hg^0 removal efficiency could be obtained in the MCO. The optimal microwave power and empty bed residence time (EBRT) in the microwave plasma catalytic oxidation were 264 W and 0.41 s, respectively. The effect of Hg^0 oxidation in the MCO was much higher than that in the MC. Microwave accentuated catalytic oxidation of mercury, and increased mercury removal efficiency. The additional use of ozone to the microwave–catalysis over Mn/zeolite led to the enhancement of mercury oxidation. Mn/zeolite catalyst was characterized by X–ray diffraction (XRD), X–ray photoelectron spectroscopy (XPS), Fourier transform infrared spectra (FT–IR), scanning electron microscopy (SEM) and the Brunauer Emmett Teller (BET) method. Microwave catalytic mercury over Mn/zeolite was dominated by a free radical oxidation route. Ozone molecules in air could enhance free radical formation. The coupling role between ozone and radicals on mercury oxidation in the MCO was formed. The MCO appears to be a promising method for emission control of elemental mercury.

Keywords: *Elemental mercury, flue gas, Mn/zeolite, microwave catalytic oxidation, characterization*

Corresponding Author:
Zaishan Wei
☎ : *+86-20-84037096*
℡ : *+86-20-39332690*
✉ : *weizaishan98@163.com*

Article History:
Received: 21 February 2014
Revised: 08 July 2014
Accepted: 11 July 2014

doi: 10.5094/APR.2015.006

1. Introduction

Mercury is a pollutant of concern due to its toxicity, volatility, persistence, and bioaccumulation in the environment (Zheng et al., 2012). Mercury is generated in the off–gas from coal–fired electric utilities, municipal waste combustors, medical waste incinerators, chlor–alkali, metal and cement plants (Ci et al., 2011). Mercury emission from coal–fired flue gas often presents in three main forms: particulate–associated [Hg(p)], gaseous divalent (Hg^{2+}) and elemental (Hg^0) (Kim et al., 2010), in which elemental mercury is the most difficult to be captured with the existing air pollution control devices (Shetty et al., 2008; Wu et al., 2011). Due to the potential mercury pollutant, elemental mercury treatment has attracted significant attention.

Conversion of Hg^0 to Hg^{2+} can be accomplished by heterogeneous catalysis or homogeneous gas phase oxidation. Magnetic zeolite composites with supported silver nanoparticles were able to capture mercury from the flue gases of an operational, full–scale, coal–fired power plant (Dong et al., 2009). Bromine chloride (BrCl) was employed to oxidize Hg^0 to $HgCl_2$ (Qu et al., 2009). Several materials have been proposed as catalysts for mercury oxidation, these materials include palladium, gold, iridium, platinum, iron, selective catalytic reduction (SCR) catalysts, fly ash, activated carbons (AC), and thief carbons (Presto and Granite, 2006; Wilcox et al., 2012). A co–benefit of SCR implementation was that it was effective at oxidizing Hg^0 to Hg^{2+} (Li et al., 2012a). The MnO_X–CeO_2/TiO_2 catalyst was highly active for Hg^0 oxidation even under SCR condition, but NH_3 consumed surface oxygen and limited Hg^0 adsorption, hence inhibited Hg^0 oxidation (Li et al., 2012b). $CuCl_2$/TiO_2 catalysts revealed high activity for mercury oxidation, the activity for mercury oxidation was significantly increased with the increase of $CuCl_2$ loading and HCl concentration (Kim et al., 2010). Hg^0 was oxidized by a heterogeneous reaction with surface Cl atom of $CuCl_2$, while oxidizing Hg^0 to $HgCl_2$ and reducing itself to CuCl (Li et al., 2013). Au/TiO_2 and Pd/Al_2O_3 catalysts on fabric filters were effective, yielding mercury oxidation ranges of 40–60% and 50–80%, respectively (Hrdlicka et al., 2008). V_2O_5/AC showed a high capability for flue gas Hg^0 capture due to catalytic oxidation of Hg^0 to Hg^{2+} by V_2O_5 (Wang et al., 2010a). Hg^0 was likely to be oxidized and retained by the oxidative elements produced on an activated carbon using zinc chloride surface through chemical activation (Hu et al., 2009). Hg^0 capture by Mn–Fe spinel could be promoted by the incorporation of Ti, Fe–Ti–Mn spinel could be magnetically separated from the fly ash (Yang et al., 2011). Using ICl to oxidize elemental mercury in coal–fired flue gas could save the consumption of iodine (Qu et al., 2010). The Hg^0 removal efficiency of titania nanotubes could exceed 90% for 100 h reaction (Wang et al., 2011). Hg^0 could be oxidized by active oxygen atom on the surface of nano–Fe_2O_3 as well as lattice oxygen in nano–Fe_2O_3 (Kong et al., 2011). Catalytic oxidation of Hg^0 transformation into Hg^{2+} could be a determining step to promote the adsorption of Hg species onto the TiO_{2-X} surface (His and Tsai, 2012). The integrated membrane delivery with catalytic oxidation systems was used to convert Hg^0 to Hg^{2+}, the conversion efficiency of Hg^0 reached 95% with Mo–Ru–Mn catalyst (Guo et al., 2012).

Non–thermal plasma catalysis is a promising technology for flue gas treatment. Microwave irradiation was applied to a

pyrolytic carbon such as activated carbon and char, enhancing the reaction of sulfur dioxide (SO_2) and nitrogen oxides (NO) with carbon (Cha and Kim, 2001). NO, SO_2 and Hg^0 oxidation efficiencies depended primarily on the radicals (OH, HO_2, O) and the active species (O_3, H_2O_2, etc.) produced by the pulsed corona discharge (Xu et al., 2009). A dielectric barrier discharge (DBD) reactor could be used to oxidize up to 80% mercury, the presence of NO_X enhanced mercury oxidation in the DBD reactor (Chen et al., 2006). Negative DC discharge induced more ozone production and a higher Hg^0 oxidation efficiency than positive DC discharge and 12 kHz AC discharge (Wang et al., 2009). Hg^0 was oxidized by utilizing both DBD of a gas mixture of Hg^0 and the injection of O_3 into the gas mixture of Hg^0 at room temperature (Byun et al., 2008). The formation of HgO_3(s) species deposited on the DBD reactor surface using O_3 injection accelerates the removal rate of Hg^0 (Byun et al., 2011). Active radicals including O, O_3 and OH all contributed to the oxidation of elemental mercury in the DBD, Hydrogen chloride could promote the oxidation of mercury due to chlorine atoms produced in the plasma process. Both NO and SO_2 had inhibitory effects on mercury oxidation, which could be attributed to their competitive consumption of O_3 and O (Wang et al., 2010b).

This work aims to study the integrated microwave with Mn/zeolite and ozone (MCO) and combined microwave with Mn/zeolite (MC) for Hg^0 oxidation. The study evaluates the role of microwave and catalyst, the coupling role of ozone and microwave catalysis on elemental mercury oxidation. This study utilizes X–ray diffraction (XRD), X–ray photoelectron spectroscopy (XPS), Fourier transform infrared spectra (FT–IR), scanning electron microscopy (SEM) and the Brunauer Emmett Teller (BET) method toward the understanding of the formation of the intermediate products and their involvement in the reaction mechanism of microwave catalytic mercury oxidation.

2. Material and Methods

2.1. Catalyst preparation

The Mn/zeolite catalyst was prepared by an incipient wetness impregnation using $Mn(NO_3)_2$ as the metal precursor, $Mn(NO_3)_2$ concentration was 0.1 mol L^{-1}. After impregnation in Ca–5A zeolite for 24 h in room temperature, the catalyst samples were dried in the vacuum drying oven at 80 °C for 2 h, and placed in the middle of muffle furnace, calcinated at 550 °C for 120 min. After cooling to room temperature, the Mn/zeolite samples were taken out for further investigations.

2.2. Experimental setup

The experimental flow loop of a microwave catalytic reactor over Mn/zeolite was shown in Figure 1. The reactor consisted of a quartz tube (10 mm i.d. and 250 mm long) with Mn/zeolite (external diameter of 3 to 4.6 mm) 10 mm in diameter and 220 mm in working height using ozone as oxidizing agent, which was set up to study elemental mercury oxidation from stimulated flue gas. Hg^0 vapor was prepared from the Hg^0 permeation unit (placed in a water bath with a temperature of 333 K) and was blended with the gases before they entered the reactor, ozone supplied from the ozone generator, were flowed upwards through the microwave reactor. Gas flow rate was monitored by the rotameter and the mass flow controllers. A constant input microwave power of 136–440 W was used and the microwave frequency was 2 450 MHz.

2.3. Analytical methods

The inlet and outlet of the bubbler were sampled for gaseous mercury in accordance with Ontario Hydro Method of U.S. EPA Method 23 and U.S. DOE. The concentrations of mercury were quantified by atomic fluorescence spectrophotometry (AFS).Gas collection was made at a velocity of 1 L min^{-1} for 5 min. Fraction analysis of soluble and insoluble mercury was performed with a series of absorption bottles that contained distilled water and an aqueous acidic solution of potassium permanganate ($KMnO_4$). The outlet gas was absorbed for the trap for divalent mercury by a bottle containing saturated KCl solution. The soluble mercury was taken to be $HgCl_2$, and the insoluble mercury was taken to be Hg^0. Ozone concentration was measured by an electro–chemical gas analyzer (AIC–800–O_3, Shenzhen aopul Co. Ltd, CHINA). XRD, XPS, FT–IR, SEM and the BET method were employed to fully characterize the Mn/zeolite. The BET method, using ASIQC0V100.2 Quantachrome (USA) instrument was used to determine the total surface area of the prepared catalysts by physisorption of nitrogen at liquid nitrogen temperature (77 K) in static mode.

3. Results and Discussion

3.1. Characterization of the Mn/zeolite

The BET area was determined to be 280.793 $m^2 g^{-1}$ for the Mn/zeolite; the total pore volume and average pore diameter of the corresponding sample were 0.094 $cm^3 g^{-1}$ and 17.047 nm, respectively (Figure 2). The Mn/zeolite had rich pore structure, and the main aperture of them was mesoporous.

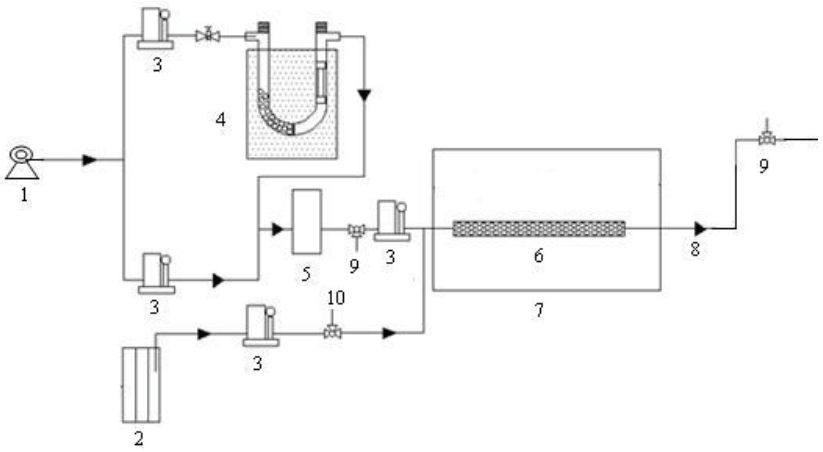

Figure 1. *Experimental flow loop of microwave catalytic elemental mercury removal over Mn/zeolite.* ***(1)*** *air compressor;* ***(2)*** *ozone generator;* ***(3)*** *flow meter;* ***(4)*** *the Hg^0 permeation unit;* ***(5)*** *the bottle of gas mixture;* ***(6)*** *catalyst bed;* ***(7)*** *microwave catalytic reactor;* ***(8)*** *outlet port;* ***(9)*** *gaseous elemental mercury sampling port;* ***(10)*** *ozone inlet sampling port.*

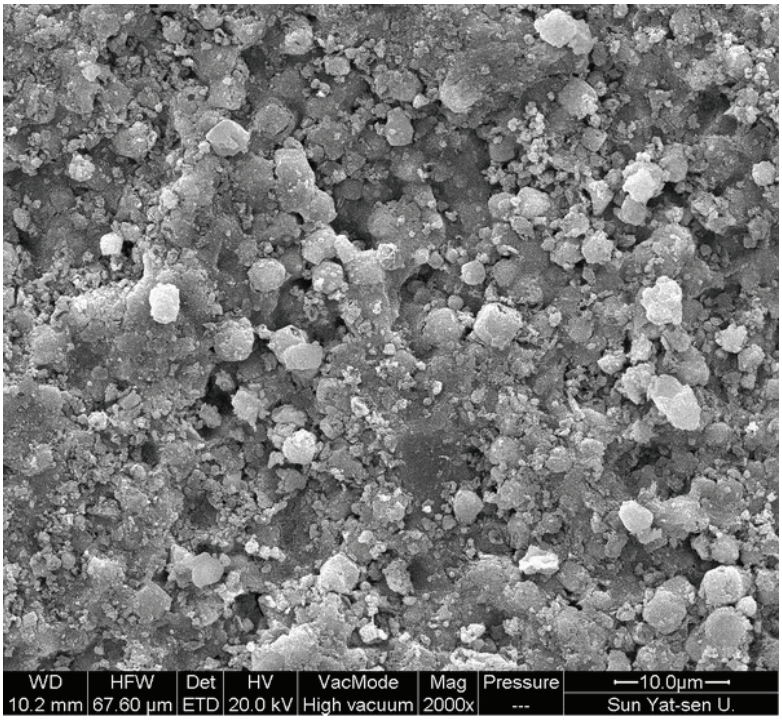

Figure 2. *SEM image of Mn/zeolite.*

The XRD pattern of Mn/zeolite catalyst was shown in Figure 3. The Al_2O_3 diffraction peaks could be observed at 2θ=15.575° and 33.225°. The sign at 32.823° could be assigned to Mn_2O_3, the diffraction peaks attributed to MnO_2 species were observed at 2θ=28.775°, 40.03° and 42.351° (Ji et al., 2002). Some Mn^{3+} and Mn^{4+} existed even before the microwave catalytic mercury reaction, the possible reason for this was that the Mn_2O_3 and MnO_2 were generated through the thermal treatment of the $Mn(NO_3)_2$ over the ambient to 550 °C.

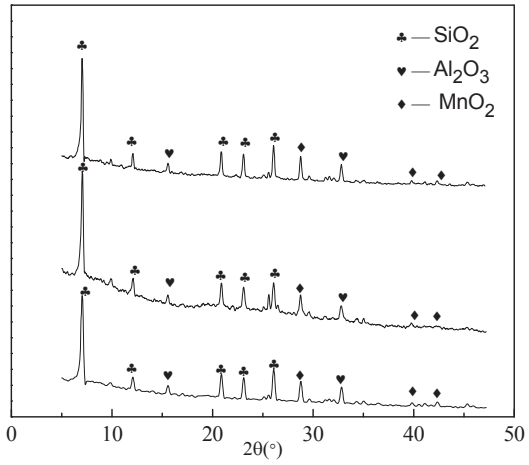

Figure 3. *XRD patterns of Mn/zeolite before and after MC and MCO of the mercury.*

Surface information on Mn/zeolite samples was analyzed by XPS. The MC, MCO and CO profile are represented by Mn/zeolite catalyst under microwave, microwave catalytic oxidation over Mn/zeolite using ozone as an oxidizing agent, catalytic oxidation over Mn/zeolite using ozone as an oxidizing agent, respectively. XPS spectra over the spectral regions of Mn2p, Hg4f and O1s are shown in Figure 4. The Mn2p region showed a band centered at 642.5 eV (fresh), 642.6 eV (MC), 642.8 eV (MCO) attributed to MnO_2. The Mn2p peak of the fresh Mn/zeolite sample consisted of two sub–peaks: Mn^{4+} peak at about 642.5 eV and Mn^{3+} peak at about 641.2 eV (Kang et al., 2007). This result may be interpreted as that Mn^{3+} was partially oxidized to Mn^{4+} with higher oxidation state after the MC or MCO reaction. The Hg4f region showed a band centered at 101.2 eV (MC), 101.9 eV (MCO), attributed to the mercuric oxide (HgO) species, with a satellite peak at 104.8 eV characteristic of elemental mercury (Hg^0). For temperatures below 450 °C, at equilibrium, nearly all mercury should exist as Hg^{2+}. Due to the excess of oxygen –containing species (O, OH, O_3 and OOH), mercuric oxide (HgO) was assumed to be the dominant form of Hg^{2+} (Presto and Granite, 2006). The O1s region showed a band centered at 532.24 eV, 532.25 eV in MC, MCO samples, corresponding to OH radial species. Hydroxyl (OH) free radical species were formed in flue gas with Hg^0/O_2, water mixtures on Mn/zeolite under microwave irradiation. The amount of total HgO on the surface of Mn/zeolite was 6.3 µg g^{-1} followed by AFS under the conditions of gas flow of 0.15 m^3 h^{-1}, microwave power of 264 W, inlet concentration of 46 µg m^{-3} Hg^0.

The FT–IR spectrum of Mn/zeolite after the MC or MCO of mercury reaction was depicted in Figure 5. The peaks at 3 413, 1 022, and 473 cm^{-1} were attributed to the stretching vibration of O–H, Si–O, Mn–O, respectively. The peaks at 544, 1 656 cm^{-1} were attributed to the vibration of Si–O, H–O relevant to H_2O groups, separately. The peak at 3 580 cm^{-1} appeared, corresponding to surface hydroxyl groups. The hydroxyl radical (OH) species in the microwave catalytic system were identified by an Agilent 1100 series high performance liquid chromatography (HPLC). Thus, it can be concluded that Hg^+ and Hg^{2+} species were formed as the reaction production from the reaction between mercury with surface oxygen species or active OH free radicals during the MC or MCO of Hg^0 reaction.

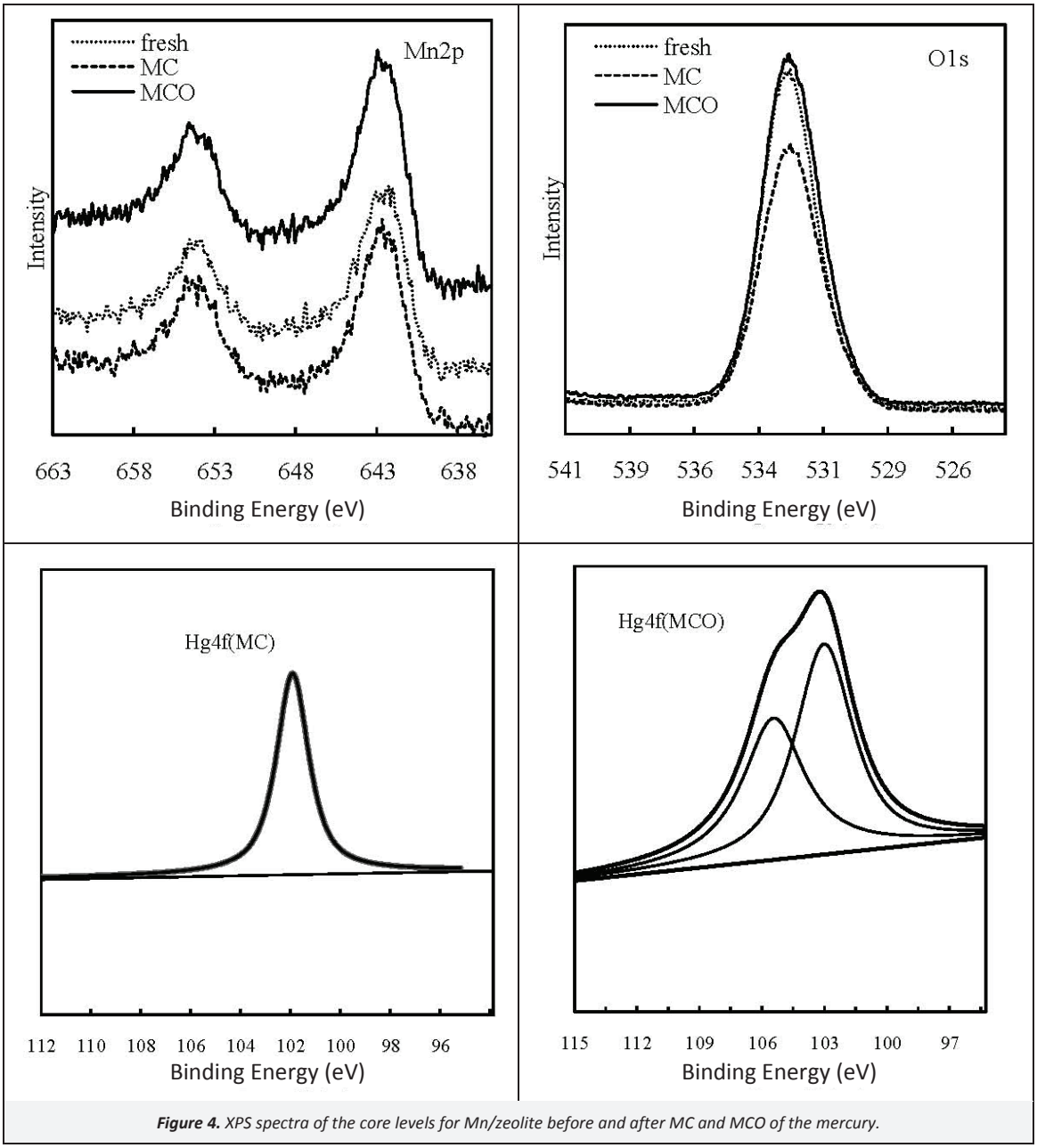

Figure 4. *XPS spectra of the core levels for Mn/zeolite before and after MC and MCO of the mercury.*

3.2. Microwave catalytic elemental mercury performance

The influence of concentration of Hg^0 in inlet on mercury oxidation was shown in Figure 6. Mercury removal efficiency gradually increased from 16 to 35.3% with increasing the concentration of Hg^0 from 33.8 to 48.3 μg m^{-3}, and then decreases to 26.3% with 85.9 μg m^{-3} in the MC process. This illustrated that the combination of microwave and Mn/zeolite catalyst allowed an efficient mercury oxidation under no oxidizing agent. The possible reason for this could be that microwave catalytic generated hydroxyl radicals play an important role in the oxidation of Hg^0 to Hg^+, Hg^{2+} (Wei et al., 2011).

When mercury and O_2, H_2O, N_2 were present in the Mn/zeolite catalyst under microwave irradiation, H_2O, N_2 and O_2 could be dissociated into atomic N, O and OH radicals. The microwave catalytic reactor in the introduction of Mn oxides showed improved oxidation of elemental mercury, which may be attributed to the formation of powerful oxidants like atomic oxygen and hydroxyl radical (Karuppiah et al., 2012). There were accelerated electrons and ions as well as radicals and neutral specie in the microwave plasma catalysis. The generated conduction band electrons were trapped by oxygen molecules, leading to the formation of radicals such as O, HOO and OH to produce active oxidizing species, usually hydroxyl radicals (OH) in presence of air, but also dissociated neutral oxygen species (O). Active radicals including O and OH all contribute to the oxidation of elemental mercury (Wang et al., 2010b). These radicals are highly reactive and rapidly react with mercury gas molecules to form HgO. Mercuric oxide formation could be understood through elemental mercury oxidation by O, OH, HO_2 radical. Oxygen or hydroperoxyl radicals formed could react with mercury to form mercuric oxide. It could be concluded that microwave catalytic mechanism for mercury removal over Mn/zeolite is dominated by a free radical oxidation route.

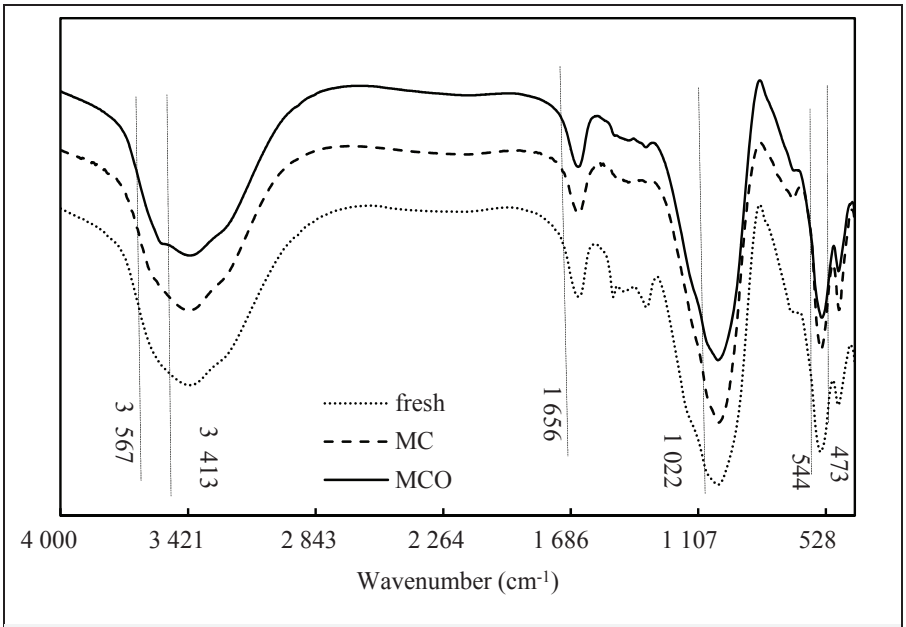

Figure 5. *FTIR spectrum of Mn/zeolite before and after MC and MCO of the mercury.*

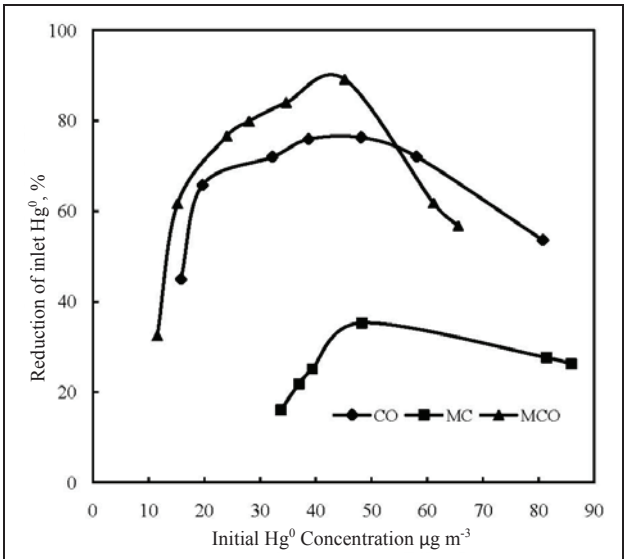

Figure 6. *Influence of inlet Hg^0 concentration of on mercury oxidation under the conditions of microwave power of 264 W at EBRT of 0.41 s.*

3.3. Microwave catalytic oxidation of mercury

Microwave catalytic oxidation of mercury performance. As was shown in Figure 6, Hg^0 removal efficiency could be up to 89.2% in the combination of microwave and Mn/zeolite using ozone as an oxidizing agent. Microwave accentuated catalytic oxidation of Hg^0, and increased Hg^0 removal efficiency from 7.5% to 16.7% with less than 54 μg m^{-3} of Hg^0 inlet in the MCO system. Hg^0 removal efficiencies of microwave catalytic oxidation were higher than those catalytic oxidation or microwave catalytic oxidation when concentration of mercury inlet was less than 54 μg m^{-3}, which were generally in the order: (MCO)>(CO)>(MC). The mercury conversion effect using MCO was lower than that using CO with more than 54 μg m^{-3} of Hg^0 inlet. The possible reason for this could be that microwave could affect the performance of the Mn/zeolite catalyst, the elimination capacity (EC) in the MCO was deceasing with the increase of inlet concentration. For comparison, in the presence of microwave irradiation and Mn/zeolite, with/without ozone in flue gas treatment process, Hg^0 removal efficiency increases from 26.5 to 67.4%, ozone promotes microwave catalytic of Hg^0. The Mn/zeolite catalyst surface reaction temperature range of microwave catalytic Hg^0 removal was 93–110 °C, obviously lower than the temperature of selective catalytic reduction (SCR), 250–400 °C.

The influence of microwave power. Figure 7 showed the influence of microwave power on mercury oxidation using ozone as the oxidizing agent and Mn/zeolite as catalyst under microwave irradiation. The conversion of Hg^0 oxidation gradually increased from 55.5% with 136 W microwave power to 88.2% with 264 W, and then decreased to 59.8% with 440 W. The experimental results showed that the optimum microwave power was supposed to be 264 W.

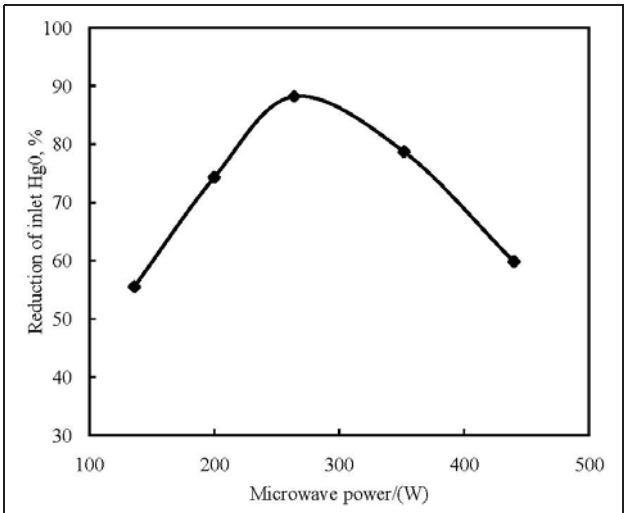

Figure 7. *Influence of mercury oxidation with different microwave powers under the conditions of flowing 46 μg m^{-3} of mercury, 128.6 mg m^{-3} of O_3 at EBRT of 0.41 s.*

The influence of empty bed residence time (EBRT). With EBRT increasing, mercury removal efficiency increased from 62.6 to 88.2%, and then slowly risen to 92.4% (Figure 8). This indicates the longer EBRT is a benefit on mercury removal in the case where the EBRT is too short to oxidize mercury to divalent (Hg^{2+}) before release. The type of Mn/zeolite catalyst and the length of the quartz tube with catalyst and oxidation agent are the key elements. From Figure 8, the optimum EBRT was 0.41 s in the microwave catalytic oxidation of mercury system, and about 88.2% mercury in the gas stream was converted.

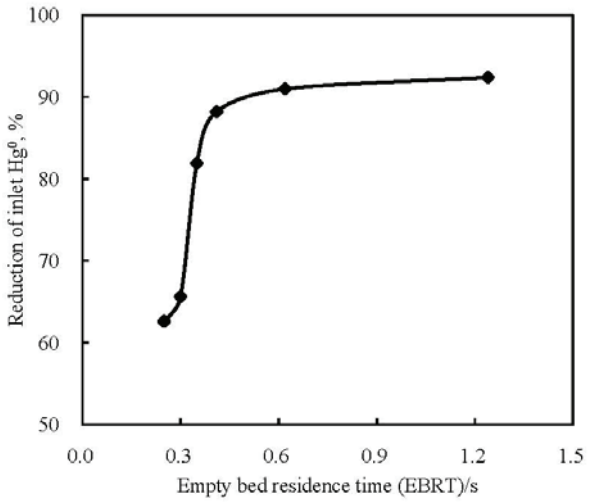

Figure 8. *Influence of empty bed residence time (EBRT) on mercury oxidation under the conditions of flowing 46 μg m^{-3} of mercury, 128.6 mg m^{-3} of O_3.*

The influence of ozone concentration. Keeping the EBRT (0.41 s), microwave power of 264 W and 46 μg m^{-3} of Hg^0 inlet fixed, the influence of ozone concentration on mercury oxidation was presented in Figure 9. Figure 9 indicated that Hg^0 removal efficiency gradually increased from 67.7 to 90.2% when the concentration of ozone inlet was increased from 42.9 to 257.1 μg m^{-3}.

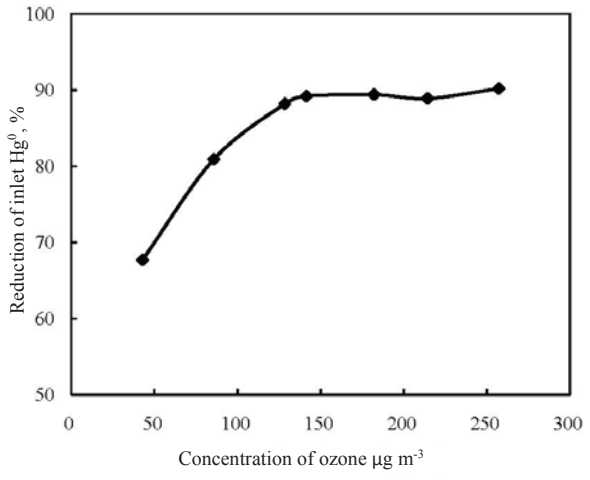

Figure 9*. Influence of inlet O_3 concentration on mercury oxidation under the conditions of EBRT of 0.41 s, microwave power of 264 W and 46 μg m^{-3} of inlet Hg^0.*

The combination of microwave with Mn/zeolite and ozone (MCO) leads to an enhancement of the mercury oxidation compared to MC system. XPS spectra indicate the formation of a stable mercuric oxide species (HgO) from the oxidation of Hg^0. In the MCO process, most of the electrical energy goes into the production of energetic electrons. These electrons trigger multiple chemical processes such as ionization, excitation and dissociation through collisions with neutral back–ground molecules (N_2, O_2, H_2O), leading to the formation of radicals such as N and O atoms, hydroxyl (OH) and hydroperoxyl (HOO), and production of N_2 and O_2 ions (Wan et al., 2011; Vandenbroucke, et al., 2014). Eventually these species, i.e., O, O_3, OH and OOH, along with electrons, contribute to the formation of divalent mercury (Kossyi et al., 1992). These free radicals would react with ozone (O_3) to generate HO_2 radicals and O_2, and then the hydroperoxyl radicals would react with O_3 to form hydroxyl radical and O_2. Ozone acts not only as electron acceptor to produce O_3• − but also as a source to generate hydroxyl radical, having a strong ability to oxidize elemental mercury. Ozone molecules in air could enhance OH radical formation. Oxidative reactions involving ozone and radicals play the dominant role in the oxidation of the mercury molecules using a microwave combined with Mn/zeolite and ozone. Hg^0 could be oxidized into HgO by active radicals including O, O_3, OH, and OOH. Oxidation of mercury with ozone produces mercuric oxide. Oxygen or hydroperoxyl radicals can react with mercury to form mercuric oxide. This observation implies that Hg oxidation prefers a pathway in which HgO was formed by oxidizing Hg to HgO by ozone and radicals.

$$H_2O, O_2 + e \xrightarrow{MCO} H^+ + OH, O, OOH \quad (1)$$

$$O_3 + OH \rightarrow HOO + O_2, HOO + O_3 \rightarrow OH + 2O_2, O_3 + H_2O \rightarrow 2OH + O_2 \quad (2)$$

$$Hg + O_3 \rightarrow HgO + O_2, Hg + O \rightarrow HgO, Hg + HO_2 \rightarrow HgO + OH \quad (3)$$

4. Conclusions

The paper revealed that the microwave catalytic oxidation or microwave catalytic over Mn/zeolite could be used for elemental mercury oxidation. Hg^0 mercury removal efficiency attained 35.3% in the MC, Hg^0 removal efficiency in the MCO was up to 92.4%. The optimal microwave power and EBRT in the MCO were 264 W and 0.41 s, respectively. The effect of Hg^0 oxidation in the MCO was much higher than that in the MC. Microwave catalytic mercury over Mn/zeolite was dominated by a free radical oxidation route. Microwave accentuated catalytic oxidation of mercury, and increased mercury removal efficiency. The additional use of ozone to the microwave–catalysis over Mn/zeolite led to the enhancement of mercury oxidation. Ozone molecules in air could enhance free radical formation. The coupling role between ozone and radicals on mercury oxidation in the MCO was formed. The microwave catalytic oxidation technology is a viable and promising method for control of the elemental mercury in flue gas.

Acknowledgments

The authors gratefully acknowledge the financial support from the Research Fund Program of Guangdong Provincial Key Laboratory of Environmental Pollution Control and Remediation Technology (2011K0010). The authors also thank Dr. H.Y. Dong and test center in Sun Yat–sen University for the catalyst characterization of XPS and FT–IR.

References

Byun, Y., Koh, D.J., Shin, D.N., 2011. Removal mechanism of elemental mercury by using non–thermal plasma. *Chemosphere* 83, 69–75.

Byun, Y., Ko, K.B., Cho, M., Namkung, W., Shin, D.N., Lee, J.W., Koh, D.J., Kim, K.T., 2008. Oxidation of elemental mercury using atmospheric pressure non–thermal plasma. *Chemosphere* 72, 652–658.

Cha, C.Y., Kim, D.S., 2001. Microwave induced reactions of sulfur dioxide and nitrogen oxides in char and anthracite bed. *Carbon* 39, 1159–1166.

Chen, Z.Y., Mannava, D.P., Mathur, V.K., 2006. Mercury oxidization in dielectric barrier discharge plasma system. *Industrial & Engineering Chemistry Research* 45, 6050–6055.

Ci, Z.J., Zhang, X.S., Wang, Z.W., Niu, Z.C., 2011. Atmospheric gaseous elemental mercury (GEM) over a coastal/rural site downwind of East China: Temporal variation and long–range transport. *Atmospheric Environment* 45, 2480–2487.

Dong, J., Xu, Z.H., Kuznicki, S.M., 2009. Mercury removal from flue gases by novel regenerable magnetic nanocomposite sorbents. *Environmental Science & Technology* 43, 3266–3271.

Guo, Y.F., Yan, N.Q., Yang, S.J., Liu, P., Wang, J., Qu, Z., Jia, J.P., 2012. Conversion of elemental mercury with a novel membrane catalytic system at low temperature. *Journal of Hazardous Materials* 213, 62–70.

His, H.C., Tsai, C.Y., 2012. Synthesis of TiO_{2-x} visible–light photocatalyst using N_2/Ar/He thermal plasma for low–concentration elemental mercury removal. *Chemical Engineering Journal* 191, 378–385.

Hrdlicka, J.A., Seames, W.S., Mann, M.D., Muggli, D.S., Horabik, C.A., 2008. Mercury oxidation in flue gas using gold and palladium catalysts on fabric filters. *Environmental Science & Technology* 42, 6677–6682.

Hu, C.X., Zhou, J.S., He, S., Luo, Z.Y., Cen, K.F., 2009. Effect of chemical activation of an activated carbon using zinc chloride on elemental mercury adsorption. *Fuel Processing Technology* 90, 812–817.

Ji, S.F., Xiao, T.C., Li, S.B., Xu, C.Z., Hou, R.L., Coleman, K.S., Green, M.L.H., 2002. The relationship between the structure and the performance of Na–W–Mn/SiO_2 catalysts for the oxidative coupling of methane. *Applied Catalysis A–General* 225, 271–284.

Kang, M., Park, E.D., Kim, J.M., Yie, J.E., 2007. Manganese oxide catalysts for NO_X reduction with NH_3 at low temperatures. *Applied Catalysis A–General* 327, 261–269.

Karuppiah, J., Karvembu, R., Subrahmanyam, C., 2012. The catalytic effect of MnO_X and CoO_X on the decomposition of nitrobenzene in a non–thermal plasma reactor. *Chemical Engineering Journal* 180, 39–45.

Kim, M.H., Ham, S.W., Lee, J.B., 2010. Oxidation of gaseous elemental mercury by hydrochloric acid over $CuCl_2$/TiO_2–based catalysts in SCR process. *Applied Catalysis B–Environmental* 99, 272–278.

Kong, F.H., Qiu, J.R., Liu, H., Zhao, R., Ai, Z.H., 2011. Catalytic oxidation of gas–phase elemental mercury by nano–Fe_2O_3. *Journal of Environmental Sciences–China* 23, 699–704.

Kossyi, I.A., Kostinsky, A.Y., Matveyev, A.A., Silakov, V.P., 1992. Kinetic scheme of the non–equilibrium discharge in nitrogen–oxygen mixtures. *Plasma Sources Science & Technology* 1, 207–220.

Li, X., Liu, Z.Y., Kim, J., Lee, J.Y., 2013. Heterogeneous catalytic reaction of elemental mercury vapor over cupric chloride for mercury emissions control. *Applied Catalysis B–Environmental* 132, 401–407.

Li, J.R., He, C., Shang, X.S., Chen, J.S., Yu, X.W., Yao, Y.J.,2012a. Oxidation efficiency of elemental mercury in flue gas by SCR De–NO_X catalysts. *Journal of Fuel Chemistry and Technology* 40, 241–246.

Li, H.L., Wu, C.Y., Li, Y., Zhang, J.Y., 2012b. Superior activity of MnO_X–CeO_2/TiO_2 catalyst for catalytic oxidation of elemental mercury at low flue gas temperatures. *Applied Catalysis B–Environmental* 111, 381–388.

Presto, A.A., Granite, E.J., 2006. Survey of catalysts for oxidation of mercury in flue gas. *Environmental Science & Technology* 40, 5601–5609.

Qu, Z., Yan, N.Q., Liu, P., Jia, J.P., Yang, S.J., 2010. The role of iodine monochloride for the oxidation of elemental mercury. *Journal of Hazardous Materials* 183, 132–137.

Qu, Z., Yan, N.Q., Liu, P., Chi, Y.P., Jia, J., 2009. Bromine chloride as an oxidant to improve elemental mercury removal from coal–fired flue gas. *Environmental Science & Technology* 43, 8610–8615.

Shetty, S.K., Lin, C.J., Streets, D.G., Jang, C., 2008. Model estimate of mercury emission from natural sources in East Asia. *Atmospheric Environment* 42, 8674–8685.

Vandenbroucke, A.M., Mora, M., Jimenez–Sanchidrian, C., Romero–Salguero, F.J., De Geyter, N., Leys, C., Morent, R., 2014. TCE abatement with a plasma–catalytic combined system using MnO_2 as catalyst. *Applied Catalysis B–Environmental* 156, 94–100.

Wan, Y.J., Fan, X., Zhu, T.L., 2011. Removal of low–concentration formaldehyde in air by DC corona discharge plasma. *Chemical Engineering Journal* 171, 314–319.

Wang, H.Q., Zhou, S.Y., Xiao, L., Wang, Y.J., Liu, Y., Wu, Z.B., 2011. Titania nanotubes–a unique photocatalyst and adsorbent for elemental mercury removal. *Catalysis Today* 175, 202–208.

Wang, J.W., Yang, J.L., Liu, Z.Y., 2010a. Gas–phase elemental mercury capture by a V_2O_5/AC catalyst. *Fuel Processing Technology* 91, 676–680.

Wang, Z.H., Jiang, S.D., Zhu, Y.Q., Zhou, J.S., Zhou, J.H., Li, Z.S., Cen, K.F., 2010b. Investigation on elemental mercury oxidation mechanism by non–thermal plasma treatment. *Fuel Processing Technology* 91, 1395–1400.

Wang, M.Y., Zhu, T.L., Luo, H.J., Tang, P., Li, H., 2009. Oxidation of gaseous elemental mercury in a high voltage discharge reactor. *Journal of Environmental Sciences–China* 21, 1652–1657.

Wei, Z.S., Zeng, G.H., Xie, Z.R., Ma, C.Y., Liu, X.H., Sun, J.L., Liu, L.H., 2011. Microwave catalytic NO_X and SO_2 removal using FeCu/zeolite as catalyst. *Fuel* 90, 1599–1603.

Wilcox, J., Rupp, E., Ying, S.C., Lim, D.H., Negreira, A.S., Kirchofer, A., Feng, F., Lee, K., 2012. Mercury adsorption and oxidation in coal combustion and gasification processes. *International Journal of Coal Geology* 90, 4–20.

Wu, S.H., Wang, S.A., Gao, J.H., Wu, Y.Y., Chen, G.Q., Zhu, Y.W., 2011. Interactions between mercury and dry FGD ash in simulated post combustion conditions. *Journal of Hazardous Materials* 188, 391–398.

Xu, F., Luo, Z.Y., Cao, W., Wang, P., Wei, B., Gao, X., Fang, M.X., Cen, K.F., 2009. Simultaneous oxidation of NO, SO_2 and Hg^0 from flue gas by pulsed corona discharge. *Journal of Environmental Sciences–China* 21, 328–332.

Yang, S.J., Guo, Y.F., Yan, N.Q., Wu, D.Q., He, H.P., Xie, J.K., Qu, Z., Jia, J.P., 2011. Remarkable effect of the incorporation of titanium on the catalytic activity and SO_2 poisoning resistance of magnetic Mn–Fe spinel for elemental mercury capture. *Applied Catalysis B–Environmental* 101, 698–708.

Zheng, Y.J., Jensen, A.D., Windelin, C., Jensen, F., 2012. Review of technologies for mercury removal from flue gas from cement production processes. *Progress in Energy and Combustion Science* 38, 599–629.